

# Exoplanets (Queloz)

Xander Byrne

Lent 2023

## 1 Formation

### 1.1 Protoplanetary Disks

When large ( $\sim 10^5$  au) clouds of gas become gravitationally unstable, they collapse, forming a massive central object surrounded by an accretion disk. When the central object exceeds  $13M_J$ , the pressure and temperature at its core is sufficient to ignite D fusion (forming a brown dwarf) and then at  $80M_J$ , H fusion: a star is born.

#### 1.1.1 Gas & Dust

The gas in the disk is mostly  $H_2$ .  $H_2$  is difficult to observe – it is symmetric and so IR-inactive. CO is IR-active and fairly abundant, so is often used as a proxy for the total disk mass, assuming a fixed CO- $H_2$  ratio. Further, CO solidifies below 17K, so it cannot be used in the cool outer disk.

If the disk is resolved, one can spatially map the radial velocity of CO absorption lines, revealing the rotation of the disk. If not, all you have is the superimposed SEDs of the star and the disk. The stellar SED is roughly a blackbody; the disk has a range of temperatures, so its SED will be a blurred blackbody spectrum. The inner edge of the disk is somewhat cooler than the star<sup>1</sup>, so the superposed spectrum is double-peaked. The intensity  $I_\nu^{\text{disk}}$  from an annulus radius  $r$  of the disk will be  $B_\nu(T)(1 - e^{-\tau_\nu})$ , where  $T$  is the disk temperature at radius  $r$ , and  $\tau_\nu$  is the optical depth to the observer.  $\tau_\nu$  is approximately given by  $\kappa_\nu \Sigma(r) / \cos i$ , where  $\Sigma(r)$  is the surface density (almost entirely due to dust) and  $i$  is the inclination angle<sup>2</sup>; for an optically thin disk  $\tau \ll 1$ . An observer will therefore receive a total intensity<sup>3</sup>:

$$I_\nu^{\text{rec}} = \int_{r_{\text{in}}}^{\infty} I_\nu^{\text{disk}} \frac{2\pi r \, dr \cos i}{D^2} = \frac{\cos i}{D^2} \int_{r_{\text{in}}}^{\infty} B_\nu(T) \underbrace{(1 - e^{-\tau_\nu})}_{\approx \tau_\nu} 2\pi r \, dr = \frac{1}{D^2} \int_{r_{\text{in}}}^{\infty} B_\nu(T) \kappa_\nu \cdot 2\pi r \, dr \Sigma(r)$$

$I_\nu$  thus approximately scales with the total disk mass; this approximation works best at large wavelengths, where the disk is optically thinnest.

The other component of a protoplanetary disk is the dust, consisting of sub- $\mu\text{m}$  solid silicate particles. Dust only makes up  $\sim 1\%$  of the mass.

---

<sup>1</sup>The star blasts out a cavity at the centre of the disk, separating it from the disk's inner edge.

<sup>2</sup> $i = 0$ : face-on.  $i = \pi/2$ : edge-on.

<sup>3</sup>Confusingly, this intensity was labelled  $F_\nu$  in the notes.

### 1.1.2 Vertical Structure

The disk can be assumed in vertical hydrostatic equilibrium. As such the gas obeys  $\frac{\partial p}{\partial z} = -\rho g_z$ :

$$\Rightarrow c_s^2 \frac{\partial \rho}{\partial z} = -\rho \Omega^2 z \quad \Rightarrow \quad \rho(z) \propto \exp\left(-\frac{z^2}{2H^2}\right) \quad \text{where } H \equiv c_s/\Omega$$

The vertical structure of the disk (through its characteristic thickness  $H$ ) is therefore related to the local thermodynamics ( $c_s$ ) and the global gravity ( $\Omega$ ). Substituting for  $c_s$  and  $\Omega$ ,

$$H = \sqrt{\frac{kT}{\mu m_p} \frac{a^3}{GM_*}} \propto T^{1/2} a^{3/2}$$

As  $T$  scales rather weakly with  $a$  (something like  $T \propto a^{-3/4}$ ),  $H$  increases with  $a$  and the gas in the disk therefore flares outwards.

### 1.1.3 Gravitational Instability

The radial momentum equation is

$$v_r \frac{\partial v_r}{\partial r} - \frac{v_\phi^2}{r} + \frac{1}{\rho} \frac{\partial p}{\partial r} + \frac{GM_*}{r^2} = 0$$

Considering oscillatory radial perturbations, e.g.  $p = p_0 + \tilde{p}e^{i(\omega t + kr)}$ , one can find<sup>4</sup>:

$$\omega^2 = \Omega_r^2 - 2\pi G\Sigma|k| + c_s^2 k^2$$

where  $\Omega_r$  is the frequency of radial oscillations; in a Keplerian disk  $\Omega_r = \Omega$ . We see that for large  $k$ , we have sound waves, and for small  $k$  the oscillations are due to the global potential, as expected. For intermediate  $k$ , the local gravitational force ( $\sim G\Sigma$ ) may be strong enough to cause  $\omega^2 < 0$  and hence perturbations to grow exponentially; the disk will be susceptible to this *gravitational instability* (GI). The quadratic on the RHS is negative for some  $k$  provided

$$c_s \Omega_r < \pi G\Sigma \quad \Rightarrow \quad Q \equiv \frac{c_s \Omega_r}{\pi G\Sigma} < 1$$

where we define the *Toomre parameter*  $Q$ . If  $Q < 1$ , the disk will be unstable to GI. For early Jupiter parameters,  $T \approx 75\text{K}$ ,  $a \approx 5\text{au}$ ,  $H/a \approx 0.05$ ,  $\Sigma \sim 10^3\text{gcm}^{-2}$ , we find  $Q \sim 5$ , suggesting that the Solar System was stable to GI: this was not how our planets formed. However, we see that  $Q \propto c_s \Omega_r \propto T^{1/2} a^{-3/2}$ , so the small population of giant planets found at large distances from their stars may have formed by GI in the cool outer regions of their PPDs.

---

<sup>4</sup>This is treated better in the Dynamics of Astrophysical Disks course

## 1.2 Core Accretion Model

A model which better explains the formation of the Solar System is the *core accretion* model:

### 1.2.1 Grain Formation

Dust particles are initially so small ( $< 1\mu\text{m}$ ) that they are easily swept around by the gas – their motion is strongly “coupled” to the turbulent motion of the gas, sweeping the dust particles into eddies. This facilitates collisions between the particles, which may then stick together electrostatically to form *dust grains* ( $> 1\mu\text{m}$ ). Sticking is particularly likely (as opposed to bouncing off each other) if the dust has some ice on it.

### 1.2.2 Decoupling, Settling, and Decoupling Again

When the grains become  $> 1\text{mm}$ , they have enough inertia that their motion is no longer completely dictated by the gas – the grains “decouple” from the gas, though they still experience drag from it. As a result, the dust eventually settles into Keplerian orbits in the midplane of the disk. The equation of motion of the grains in the  $z$ -direction is

$$\frac{\partial^2 z}{\partial t^2} = -\frac{1}{\tau_f} \frac{\partial z}{\partial t} - \Omega^2 z$$

where  $\tau_f$  is the frictional timescale of gas drag force on the grains. This equation is that of a damped harmonic oscillator: if  $\tau_f \rightarrow \infty$  then there is no drag and the grains perform inclined Keplerian orbits; if  $\tau_f = 0$  then we require  $\partial z / \partial t = 0$  and no settling occurs. These limits are both unrealistic; Epstein<sup>5</sup> found that a good model for spherical grains is

$$\tau_f = \frac{\rho_s R_s}{\rho_g c_s} = \frac{\rho_s R_s}{\rho_g H \Omega}$$

where  $\rho_g$  and  $\rho_s$  are the densities of the gas and the solid grains and  $R_s$  is the grain radius. One finds that dust settles onto the midplane very quickly<sup>6</sup> following decoupling.

After settling in the midplane, the *azimuthal* drag forces first circularise the grains’ orbits. Over slightly longer timescales, the azimuthal gas drag robs the grains of energy and AM, causing them to fall inwards. This azimuthal drag only exists because the gas orbits at sub-Keplerian velocities, due to the outward gas pressure gradients offsetting some of the central gravitational force, reducing the overall centripetal force on the gas. The grains (apparently?) are not affected by these pressure gradients, so orbit at Keplerian speeds, experiencing a significant headwind ( $\sim 100\text{ms}^{-1}$ ) as they pass through the gas.

The drag experienced by the grains is so significant that if they don’t grow quickly enough they should fall to the centre in a matter of centuries. If they can quickly grow to a size of  $\gtrsim 1\text{m}$  then their inertia becomes large enough that even the gas drag becomes negligible (this can be thought of as a second decoupling), but the theoretical difficulties for such quick growth lead this to be known as the *metre-size barrier* or *cm-size problem*. It is unclear exactly how grains get from  $\sim\text{mm}$  size to  $\sim 100\text{m}$  size, but clearly they must do somehow! When they do so, the bodies are called *planetesimals*.

---

<sup>5</sup>Not that one

<sup>6</sup>The notes give  $\sim 10^7\text{yr}$ ; others suggest shorter timescales of  $\sim 10^5\text{yr}$  or even  $\sim 10^3\text{yr}$

### 1.2.3 Planetesimal Growth

Planetesimals grow by collision with each other and by accreting grains, forming *planetary embryos*. The latter process can be modelled as the planetesimal, of radius  $R$  and mass  $M$  streaming through a medium with a density of solid particles  $\rho$  at relative speed  $v_{\text{rel}}$  and accreting everything that hits them:

$$\frac{dM}{dt} = f_g \cdot \pi R^2 \rho v_{\text{rel}}$$

where  $f_g \geq 1$  is a factor due to the phenomenon of gravitational focusing, whereby particles with impact parameters  $> R$  can end up hitting the planet as they are drawn in by the planetesimal's gravity. To calculate this parameter, let  $b$  be the maximum impact parameter at which a particle would not escape the planetesimal when travelling at  $v_{\text{rel}}$ , i.e. its periapsis is the planetesimal's radius  $R$ . To find  $b$  in terms of other parameters of the problem, we use conservation of angular momentum and energy to give

$$bv_{\text{rel}} = Rv_I; \quad \frac{1}{2}v_{\text{rel}}^2 = \frac{1}{2}v_I^2 - \frac{GM}{R} \quad \Rightarrow \quad b^2 = R^2 \left( 1 + \frac{2GM}{Rv_{\text{rel}}^2} \right) = R^2 \left( 1 + \frac{v_{\text{esc}}^2}{v_{\text{rel}}^2} \right)$$

where  $v_I$  is the particle's speed at closest approach (in this case, tangential impact), and we recognise  $v_{\text{esc}}^2 = 2GM/R$  as the square of the escape velocity at the planet's surface. The effective cross-section of the planetesimal is then altered from  $\pi R^2$  to  $\pi b^2$ , so we identify  $f_g = 1 + v_{\text{esc}}^2/v_{\text{rel}}^2$ .

We can use this to estimate the mass growth over time in different regimes. If the planetesimal is small or  $v_{\text{rel}}$  is large then we will have  $f_g \approx 1$ , so  $dM/dt \propto R^2 \propto M^{2/3}$ . In the opposite regime,  $f_g \approx v_{\text{esc}}^2/v_{\text{rel}}^2 \propto M/R$ , so  $dM/dt \propto MR \propto M^{4/3}$ . We can define a mass-doubling timescale  $\tau = M(dM/dt)^{-1}$ , seeing that this goes as  $M^{-1/3}$  and  $M^{1/3}$  in the respective regimes. The mass growth accelerates in both regimes, but especially after the mass is such that  $v_{\text{esc}} > v_{\text{rel}}$ . At this point, though there will be an ensemble of planetesimals of various sizes, the few that are lucky enough to cross this threshold will very quickly gobble up the rest of the material in the disk thanks to gravitational focusing, forming planetary embryos of  $\sim 10^5\text{m}$ . Very little material is left for the unlucky planetesimals, which will forever remain as such (e.g. Phobos & Deimos; Arrokoth), never to achieve their planetary potential. This dominance of a small number of rapidly-growing bodies is known as *oligarchic growth*.

The matter swept up by these oligarchic embryos comes from within an annulus of the disk, characterised by the region within which the embryo's gravity dominates over both that of the star as well as centrifugal effects. If  $M \ll M_*$ , then L1 and L2 are roughly equidistant from the planet at a distance  $R_H \ll a$ , which can be found by setting the combined gravitational forces of the star and the planet at L2 equal to the centrifugal force there:

$$\Omega^2(a + R_H) = \frac{GM_*}{(a + R_H)^2} + \frac{GM}{R_H^2} \quad \Rightarrow \quad \frac{3GM_*}{a^3} R_H \approx \frac{GM}{R_H^2} \quad \Rightarrow \quad R_H \approx \left( \frac{M}{3M_*} \right)^{1/3} a$$

Planetesimals in the disk at this stage move on Keplerian orbits, rather than dispersively. As such the relative velocity of a planetesimal at radius  $a + \Delta a$  from the star is approximately

$$v_{\text{rel}} = a\Omega(a) - (a + \Delta a)\Omega(a + \Delta a) \approx \frac{1}{2}\Omega\Delta a$$

where we have used the fact that  $a\Omega \propto a^{-1/2}$ . As such we can write

$$\frac{v_{\text{esc}}^2}{v_{\text{rel}}^2} \approx \frac{2GM}{R} \cdot \frac{4a^3}{GM_*\Delta a^2} = 24 \frac{R_H^3}{R\Delta a^2} \propto \left(\frac{R_H}{\Delta a}\right)^2 \frac{R_H}{R}$$

so  $R_H$  is a convenient length scale to use, for instance, for simulations.

Planetary embryos continue to grow until they have cleared their “feeding zone”, which turns out to be an annulus of within  $\approx \pm 4R_H$  of the embryo. When this feeding is complete, all the nearby planetesimals have been accreted and the embryo becomes isolated in a gap in the disk. Its mass at this stage, the *isolation mass*, is given by

$$M_{\text{iso}} \approx 2 \cdot 2\pi a \cdot 4R_H \cdot \Sigma(a)$$

With  $R_H \propto a$  and data suggesting  $\Sigma(a) \sim a^{-3/2}$ , this suggests that closer planets should end up being smaller, simply because their orbits are shorter. There are further complications with there likely being a higher surface density beyond the ice line (between Mars and Jupiter in the Solar System), so  $\Sigma(a)$  is likely to be a more complicated function. With the fast mass growth rates discussed above, embryos likely reach their isolation masses within only  $\sim 10^6$ yr.

#### 1.2.4 Envelope Accretion

A planetary embryo may form the core of a rocky planet, or if there is a lot of gas left in the disk it may accrete the gas into a surrounding envelope, forming a gas giant planet. The gas is blown away from the inside by the active new star, so there is only  $\sim 10^7$ yr to accrete gas.

Similarly to planetesimal growth, the envelope accretion can be modelled by

$$\frac{dM}{dt} \sim \pi R_{\text{gc}}^2 \rho_g v_{\text{rel}} \sim \frac{\Sigma}{H} \Omega R_{\text{gc}}^2$$

where  $R_{\text{gc}}$  is the gas accretion radius (described shortly), and we have substituted  $\rho_g \sim \Sigma/H$  and  $v_{\text{rel}} \sim \Omega R_{\text{gc}}$ . Now for gas accretion to occur, the gas must pass within a radius such that the embryo’s gravity dominates over not only the star’s gravity and centrifugal force (as  $R_H$ ), but also the gas pressure. As such the gas can only be accreted if it comes within both  $R_H$  and the *Bondi radius*,  $R_B \sim GM/c_s^2$ . Thus  $R_{\text{gc}} = \min(R_H, R_B)$ .

Clearly, gas accretion can only occur if the mean velocity of the gas (of order  $c_s \sim H\Omega$ ) is less than the escape velocity at the surface of the embryo:

$$H\Omega < \sqrt{\frac{2GM}{R}} \quad \Rightarrow \quad M > \frac{RH^2}{2G} \frac{GM_*}{a^3} \quad \Rightarrow \quad M > \frac{H^2 M_* R}{2a^3}$$

However the cutoff here is  $\sim 0.1M_{\text{Moon}}$ , so no problems there.

Another potential problem is the energy released by the falling gas. If this energy cannot be radiated away efficiently enough, then the gas will heat up, increase mean velocity, and escape; perhaps this happened somewhat with Uranus and Neptune. However, if the planet core is large enough ( $\gtrsim 16M_E$ ), atmospheric models suggest that the envelope collapses (somehow?) and accretion becomes rapid; perhaps this happened with Jupiter and Saturn.

### 1.3 Migration

Forming planets interact with the remains of the disk: inner regions are orbiting the star more quickly; outer regions more slowly; the planet exchanges angular momentum with the disk.

Consider a planetesimal ( $m$ ) in the disk passing on the outside of a large planetary embryo ( $M$ ) at impact parameter  $x$  and relative azimuthal velocity  $v_y = -v_0 \approx -\frac{1}{2}\Omega x$ . Assuming only a weak interaction, such that  $x$  and  $v_y$  are approximately constant, the horizontal ( $x$ -directed) acceleration of the body will be approximately

$$\dot{v}_x \approx -\frac{GM}{x^2 + v_0^2 t^2}$$

with  $x$  and  $v_0$  approximately constant, this gives a change in  $x$ -velocity and deflection angle:

$$\Delta v_x \approx \int_{-\infty}^{\infty} \frac{GM}{x^2 + v_0^2 t^2} dt = \frac{\pi GM}{x v_0} \quad \Rightarrow \quad \delta \approx \frac{\pi GM}{x v_0^2} \approx \frac{4\pi GM}{\Omega^2 x^3} = 4\pi \frac{M}{M_*} \left(\frac{a}{x}\right)^3$$

Apparently,  $v_y$  also changes by  $\Delta v_y = v_0(1 - \cos \delta) \approx v_0 \delta^2$ , that is, the embryo drags the planetesimal forward with it slightly, increasing its (relative, negative) velocity. The gain in angular momentum of the planetesimal is then

$$\Delta J \approx m a v_0 \left[ 4\pi \frac{M}{M_*} \left(\frac{a}{x}\right)^3 \right]^2 \approx m a \frac{1}{2} \Omega x \cdot 16\pi^2 \left(\frac{M}{M_*}\right)^2 \left(\frac{a}{x}\right)^6 = 8\pi^2 m a^2 \Omega \left(\frac{M}{M_*}\right)^2 \left(\frac{a}{x}\right)^5$$

This angular momentum is robbed from the planet, which therefore is encouraged to inspiral. For a continuum, the  $\Delta J$  on the planet due to the outer portion of the disk may be written

$$\Delta J_{\text{outer}} \approx -8\pi^2 a^7 \Omega \left(\frac{M}{M_*}\right)^2 \int_{\Delta r}^{\infty} 2\pi x \Sigma(x) dx \cdot x^{-5}$$

The integrand has a large negative power of  $x$ , so we can approximate  $\Sigma(x)$  as taking its value in this region of the disk and bring it outside the integral; we then find

$$\Delta J_{\text{outer}} \approx -16\pi^3 a^4 \Omega \Sigma \left(\frac{M}{M_*}\right)^2 \left(\frac{a}{\Delta r}\right)^3$$

$\Delta J_{\text{inner}}$  has the same form but with a plus sign. A net torque comes from the difference in  $\Sigma$  across the gap; approximating  $\Sigma(a) \propto a^{-\beta}$  as a power law, we will have  $d\Sigma/da = -\beta\Sigma/a$ , and hence

$$\Delta J_{\text{tot}} \sim 16\pi^3 a^4 \Omega \left(\frac{M}{M_*}\right)^2 \left(\frac{a}{\Delta r}\right)^3 \left[ \frac{\beta \Sigma}{a} \cdot 2\Delta r \right] = 32\pi^3 \beta a^4 \Omega \Sigma \left(\frac{M}{M_*}\right)^2 \left(\frac{a}{\Delta r}\right)^2$$

Note that this is greater than 0 because the inner disk has a greater surface density; the net effect is thus to push the planet out, as it yanks angular momentum from the inner-orbiting planetesimals. To obtain a torque, we divide the net angular momentum change by the timescale over which the interaction occurs,  $\sim 2\pi/\Omega$ , giving<sup>7</sup>

$$\mathcal{T} \approx 16\pi^2 \beta a^4 \Omega^2 \Sigma \left(\frac{M}{M_*}\right)^2 \left(\frac{a}{\Delta r}\right)^2$$

In reality, the migration effect is the other way around, due to complicated resonance effects and non-monotonicities in  $\Sigma(a)$ . One also finds migration timescales of  $10^4 - 10^5$  yr – the planets should fall into their star almost immediately! There's obviously something else going on here, but clearly it's very easy to move a planet!

<sup>7</sup>Queloz ignores the prefactor but as it's  $\sim 10^2$  that seems naive.

## 1.4 Timing

Planet formation can be timed with radioactive dating, under the assumption that the radioactive elements were formed at the time of formation of the Solar System. A particularly useful isotope for this is  $^{26}\text{Al}$ , which  $\beta^+$ -decays into  $^{26}\text{Mg}$  with a half-life of  $\tau = 717\text{kyr}$ , similar to planet formation timescales. We therefore have

$$\begin{aligned} {}^{26}\text{Mg}(\text{now}) &= {}^{26}\text{Mg}(0) + {}^{26}\text{Al}(0)(1 - e^{-t/\tau}) \\ \Rightarrow \frac{{}^{26}\text{Mg}(\text{now})}{{}^{24}\text{Mg}(\text{now})} &= \frac{{}^{26}\text{Mg}(0)}{{}^{24}\text{Mg}(0)} + \frac{{}^{27}\text{Al}(\text{now})}{{}^{24}\text{Mg}(\text{now})} \frac{{}^{26}\text{Al}(0)}{{}^{27}\text{Al}(0)} (1 - e^{-t/\tau}) \end{aligned}$$

where the LHS is often written  $\delta^{26}\text{Mg}$ , and we have used the fact that  $^{24}\text{Mg}$  is stable and hence  ${}^{24}\text{Mg}(\text{now}) = {}^{24}\text{Mg}(0)$ . The “now” ratios are easily measured, and the primordial aluminium ratio is a constant, so if we have a rock sample we can measure the time between the formation of the Solar System and the formation of the rock (assuming no transfer of material since).

## 2 Detection

### 2.1 Keplerian Orbits

Consider two bodies of masses  $M_1$  and  $M_2$ . Their accelerations are

$$\ddot{\mathbf{r}}_1 = \frac{GM_2}{|\mathbf{r}_2 - \mathbf{r}_1|^3}(\mathbf{r}_2 - \mathbf{r}_1) \quad \ddot{\mathbf{r}}_2 = \frac{GM_1}{|\mathbf{r}_2 - \mathbf{r}_1|^3}(\mathbf{r}_1 - \mathbf{r}_2)$$

Changing to the variables  $\mathbf{r} = \mathbf{r}_2 - \mathbf{r}_1$  and  $\mathbf{R} = (M_1\mathbf{r}_1 + M_2\mathbf{r}_2)/(M_1 + M_2)$ , we obtain

$$\ddot{\mathbf{r}} = -\frac{G(M_1 + M_2)}{r^3}\mathbf{r} \quad \ddot{\mathbf{R}} = \mathbf{0}$$

so the displacement vector obeys an inverse-square law and the centre of mass coasts at constant velocity. The vector  $\mathbf{h} \equiv \mathbf{r} \times \dot{\mathbf{r}}$  is a constant, as  $\dot{\mathbf{h}} = \dot{\mathbf{r}} \times \dot{\mathbf{r}} + \mathbf{r} \times \ddot{\mathbf{r}} = \mathbf{0}$ . As such the trajectory of  $\mathbf{r}$  (and hence those of  $\mathbf{r}_1$  and  $\mathbf{r}_2$ ) is confined to a plane. We prescribe in this plane the polar coordinates  $r$  and  $\theta$ , where  $\mathbf{r} = r\hat{\mathbf{e}}_r$  and so  $\dot{\mathbf{r}} = \dot{r}\hat{\mathbf{e}}_r + r\dot{\theta}\hat{\mathbf{e}}_\theta$ ; hence  $h = r^2\dot{\theta}$  is conserved. The rate at which an orbit sweeps out area,  $\frac{1}{2}r^2\dot{\theta} \equiv h/2$  is therefore constant ( $\mathfrak{R2L}$ ).

The relative acceleration in these coordinates is

$$\ddot{\mathbf{r}} = (\ddot{r} - r\dot{\theta}^2)\hat{\mathbf{e}}_r + (2\dot{r}\dot{\theta} + r\ddot{\theta})\hat{\mathbf{e}}_\theta$$

We must therefore have  $\ddot{r} - h^2/r^3 = -G(M_1 + M_2)/r^2$ . This is solved via the substitution  $u = 1/r$ , following which one can find an expression for  $r(\theta)$ :

$$r(\theta) = \frac{h^2}{G(M_1 + M_2)} \frac{1}{1 + e \cos \theta}$$

where  $e$  is an integration constant, and we have fixed a second integration constant so that  $\theta = 0$  corresponds to periapsis; then  $\theta$  is called the *true anomaly*. Substituting for  $x$  and  $y$  shows these curves to be conic sections; for  $0 \leq e < 1$  they are ellipses of eccentricity  $e$ . Further investigation shows these to have semi-axes given by

$$a = \frac{1}{1 - e^2} \frac{h^2}{G(M_1 + M_2)}, \quad b = a\sqrt{1 - e^2} \quad \Rightarrow \quad r(\theta) = \frac{a(1 - e^2)}{1 + e \cos \theta}$$



The area of an ellipse is  $\pi ab$ , so the period can be found using the area sweeping rate:

$$P = \frac{\pi ab}{h/2} = \frac{2\pi a^2 \sqrt{1-e^2}}{h} = \frac{2\pi a^{3/2}}{\sqrt{G(M_1 + M_2)}}$$

and thus  $P \propto a^{3/2}$  ( $\mathfrak{K}_3\mathfrak{L}$ ).

### 2.1.1 Projection

These orbits are observed projected on the sky plane: whereas the coordinates of the orbit may be expressed in terms of  $(x, y, z) = (r \cos \theta, r \sin \theta, 0)$  in the orbital plane, the projection on the sky plane is best expressed in different coordinates  $(X, Y, Z)$ , where the  $XY$ -plane is the sky plane and the  $Z$ -direction is towards Earth. Projecting an orbit requires 3 angles<sup>8</sup>:

- The *inclination angle*  $i$  is the angle between the orbital plane and the sky plane.
- The *argument of periapsis*  $\omega$  swings the ellipse around *in the orbital plane*;  $\omega$  has no effect on a circular orbit.
- The *longitude of the ascending node*  $\Omega$  gyrates the ellipse around *in the sky plane*.  $\Omega$  does not affect the  $Z$ -coordinate, and only adds a phase in the  $XY$ -plane. It is thus dependent on our (arbitrary) choice of coordinates for the sky plane; we choose to set  $\Omega = \pi$ .

Applying this projection to the  $(x, y, z)$  coordinates, one finds in terms of  $r(t)$  and  $\theta(t)$ :

$$X(t) = -r \cos(\theta + \omega) \quad Y(t) = -r \sin(\theta + \omega) \cos i \quad Z(t) = r \sin(\theta + \omega) \sin i$$

## 2.2 Radial Velocity

The radial velocity method detects the presence of a planet around a star through the star's radial velocity, which Doppler shifts the star's spectral lines. A photon emitted at wavelength  $\lambda_0$  from a body moving at radial velocity  $v_r$  will be measured at rest to have wavelength

$$\lambda = \lambda_0 \left(1 + \frac{v_r}{c}\right) \quad \Rightarrow \quad \frac{\Delta \lambda}{\lambda_0} = \frac{v_r}{c}$$

where we have neglected general relativistic effects and terms of order  $\mathbf{v}^2/c^2$ . Identifying body 1 in the above as the star (mass  $M_*$ ) and body 2 as the planet ( $M$ ), the radial velocity of the star is given by  $v_r \equiv \dot{\mathbf{r}}_1 \cdot \hat{\mathbf{e}}_Z$ . In terms of  $\mathbf{R}$  and  $\mathbf{r}$ ,

$$\dot{\mathbf{r}}_1 = \dot{\mathbf{R}} - \frac{M}{M_* + M} \dot{\mathbf{r}} \quad \Rightarrow \quad \dot{\mathbf{r}}_1 \cdot \hat{\mathbf{e}}_Z = V - \frac{M}{M_* + M} \dot{Z}$$

where  $V$  is the (constant) radial velocity of the centre of mass, and  $Z(t)$  was given above. Differentiating  $r(\theta)$  with respect to time one finds  $\dot{r} = e \sin \theta r \dot{\theta} / (1 + e \cos \theta)$ . Thus

$$\dot{Z} = \left[ \dot{r} \sin(\theta + \omega) + r \dot{\theta} \cos(\theta + \omega) \right] \sin i = \underbrace{r \dot{\theta}}_{h/r} \left[ \frac{e \sin \theta \sin(\theta + \omega)}{1 + e \cos \theta} + \cos(\theta + \omega) \right] \sin i$$

---

<sup>8</sup>See <https://orbitalmechanics.info> for a nice visualisation.



$$\begin{aligned}
&= h \frac{1 + e \cos \theta}{a(1 - e^2)} \left[ \frac{e \sin \theta \sin(\theta + \omega)}{1 + e \cos \theta} + \cos(\theta + \omega) \right] \sin i \\
&= \frac{h}{a(1 - e^2)} \underbrace{\left[ e \sin \theta \sin(\theta + \omega) + e \cos \theta \cos(\theta + \omega) \right]}_{e \cos \omega} + \cos(\theta + \omega) \sin i \\
&= \frac{2\pi}{P} \frac{a}{\sqrt{1 - e^2}} [e \cos \omega + \cos(\theta + \omega)] \sin i
\end{aligned}$$

So finally, the total radial velocity as a function of  $\theta$  is

$$v_r = V - \frac{M}{M_* + M} \frac{2\pi}{P} \frac{a \sin i}{\sqrt{1 - e^2}} [e \cos \omega + \cos(\theta + \omega)]$$

The radial velocity will then oscillate sinusoidally in  $\theta$  about  $V$ . The oscillation of the radial velocity in *time* is quasi-sinusoidal but generally has no closed-form solution; one can however easily fit  $e$ ,  $\omega$ , and  $P$  (hence  $a$ ) to a library of compiled profiles<sup>9</sup>. In practice, the Earth’s motion around the Sun adds a 1-year modulation, which must be corrected by a “barycentric correction”.

The amplitude of the oscillation is then proportional to  $M \sin i / (M_* + M) \approx M \sin i / M_*$ . It is thus impossible to disentangle  $M$  and  $\sin i$  from RV measurements alone; planetary masses are often quoted as  $M \sin i$ . This is not as bad an assumption as it might seem; spherical geometry gives the probability that the system is inclined at an angle between  $i$  and  $i + di$  as simply  $\sin i \, di$  ( $i \in [0, \pi/2]$ ), so the mean value of  $\sin i$  is then  $\langle \sin i \rangle = \int_0^{\pi/2} \sin i \sin i \, di = \pi/4 \approx 0.79$ , so  $M \sin i$  will actually be a decent approximation of  $M$  (by astronomers’ standards...).

### 2.2.1 Stellar Noise

Aside from any noise emerging from the instruments, the star may further upset the measurements. Rotation of the star will mean that the star’s spectral lines already have a distribution of initial redshifts depending on where in the stellar disk each photon is emitted from. Further, the atmospheres of cool stars are convective, so parcels of gas will be moving inwards and outwards in the star at significant velocity, potentially adding further shifts.

## 2.3 Transits

Recall that in  $(X, Y, Z)$  coordinates:

$$X(t) = -r \cos(\theta + \omega) \quad Y(t) = -r \sin(\theta + \omega) \cos i \quad Z(t) = r \sin(\theta + \omega) \sin i$$

where we see that the earlier choice  $\Omega = 0$  orients the  $XY$  part of orbit as an ellipse aligned with the  $X$  and  $Y$  axes, with semi-axes  $r(t)$  and  $r(t) \cos i$ . If  $i$  is close to  $\pi/2$ , then  $(X, Y)$  can get pretty close to  $(0, 0)$  – that is,  $\mathbf{r}$  will be almost completely radial ( $Z$ -direction) and the planet and star will be aligned with our line of sight: a transit will occur.

<sup>9</sup>See <https://astro.unl.edu/naap/esp/animations/radialVelocitySimulator.html> to play around.

### 2.3.1 Impact Parameter

The closest that  $(X, Y)$  gets to  $(0, 0)$  will be approximately<sup>10</sup> when  $X = 0$ , i.e. when  $\theta = \pi/2 - \omega$ ; an occultation will occur roughly  $\pi$  later when  $\theta = 3\pi/2 - \omega$ . At the point of transit,

$$r = \frac{a(1 - e^2)}{1 + e \cos(\pi/2 - \omega)} = \frac{a(1 - e^2)}{1 + e \sin \omega} \quad \Rightarrow \quad Y = -\frac{a(1 - e^2) \cos i}{1 + e \sin \omega}$$

The dimensionless *impact parameter*<sup>11</sup>  $b$  is the number of stellar radii by which the planet misses the centre of the stellar disk in transit:

$$b \equiv \frac{Y_{(X=0)}}{R_*} = \frac{a}{R_*} \frac{(1 - e^2) \cos i}{1 + e \sin \omega}$$

### 2.3.2 Transit Probability

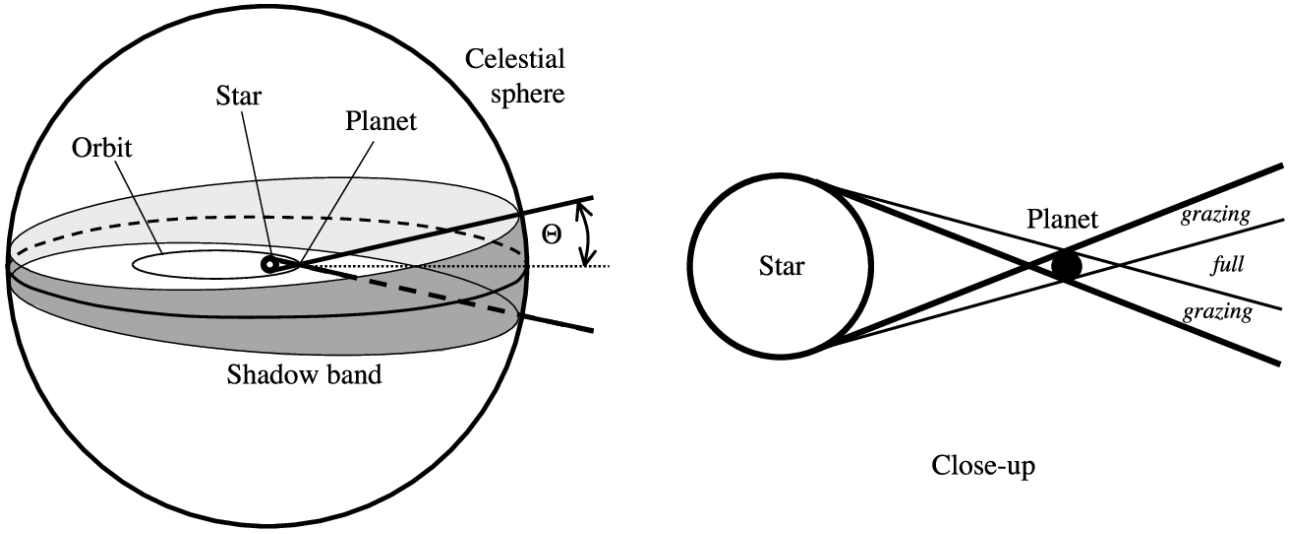


**Figure 1 | Transit Geometry.** If the observer is within the shadow band of opening angle  $\Theta(\omega)$ , then they will see a transit.

Often we make an RV measurement (obtaining  $e$  and  $\omega$ ) and want to know how likely the planet is to transit the star (i.e. that  $i$  allows a transit). Figure 1 shows that the opening angle  $\Theta$  of the shadow band of the system depends on the  $\omega$  from which you view the transit. It can also be easily shown that this shadow angle is given by<sup>12</sup>

$$\sin \Theta = \frac{R_* + R}{r_{(X=0)}} = \frac{R_* + R}{a} \cdot \frac{1 + e \sin \omega}{1 - e^2}$$

Now if nothing is known about  $i$  then its probability distribution is  $\sin i$ . Thus the probability that a system with a known  $e$  and  $\omega$  can transit is

$$P(\text{transit}|e, \omega) = \int_{\pi/2 - \Theta}^{\pi/2} \sin i \, di = \sin \Theta = \frac{R_* + R}{a} \cdot \frac{1 + e \sin \omega}{1 - e^2}$$

<sup>10</sup>This approximation only becomes remotely bad when the orbits are very very eccentric

<sup>11</sup>No idea why they call it this, it's not really an impact parameter, not least because it's dimensionless...

<sup>12</sup>Here we are talking about a *grazing* transit; for a full transit, simply replace  $R_* + R$  with  $R_* - R$ . In most cases  $R_* \gg R$  so it doesn't matter much. For occultations, replace  $\sin \omega$  with  $-\sin \omega$ .

For a population of planets of known  $e$ , but a range of  $\omega$  (which we would expect to be evenly distributed over  $[0, 2\pi]$ ), the fraction of them that would be expected to transit is

$$P(\text{transit}|e) = \int_0^{2\pi} P(\text{transit}|e, \omega) \frac{d\omega}{2\pi} = \frac{R_* + R}{a} \cdot \frac{1}{1 - e^2}$$

These probabilities pretty much just depend on  $R_*$  and  $a$ , and are generally very small:

$$\frac{R_*}{a} = 0.005 \left( \frac{R_*}{R_\odot} \right) \left( \frac{a}{1 \text{ au}} \right)$$

### 2.3.3 Timing

As  $R_* \gg R$ , the planet's path across the stellar disk can be approximated as a straight line between  $X = \pm R_* \sqrt{1 - b^2}$ , with  $Y$  being a constant at  $-bR_*$ . Four important times, labelled I through IV, are illustrated in Figure 2. Generally, to calculate the *duration of ingress/egress*  $\tau$  and the transit duration  $T$  we would need to calculate the values of  $\theta_{\text{I-IV}}$  and integrate  $\dot{\theta} = r^2/h$  over this range. Assuming a circular orbit for simplicity, the angular velocity of the planet is  $2\pi/P$ , and the angle between ingress and egress is approximately  $2R_* \sqrt{1 - b^2}/a$ . Thus

$$T \approx \sqrt{1 - b^2} \frac{R_* P}{\pi a}$$

We see that  $T \propto R_* P \propto 1/a$ . Recall from  $\mathfrak{R3}\mathfrak{L}$  that  $P \propto M_*^{-1/2} a^{3/2} \Rightarrow a \propto M_*^{1/3} P^{2/3}$ , so  $T \propto R_* M_*^{-1/3} P^{1/3} \propto P^{1/3} \rho_*^{-1/3}$ . So weirdly, the stellar density can be measured with  $T$ .

At the same angular speed, we therefore have

$$\frac{2R_* \sqrt{1 - b^2}/a}{T} = \frac{2R/a}{\tau} \Rightarrow \tau = \frac{R}{R_* \sqrt{1 - b^2}} T = \frac{RP}{\pi a}$$

A detailed calculation (with generally eccentric orbits) gives that the occultation occurs

$$\Delta t \approx \frac{1}{2} P \left( 1 + \frac{4}{\pi} e \cos \omega \right)$$

after the transit. Measurements then give the quantity  $e \cos \omega$ , which is often given as an estimate of the eccentricity, in the absence of other information.

### 2.3.4 Light Curves & Transit Spectra

When the planet and the star are both in full view, the flux will be  $F_*(t) + F_p(t)$ . When the planet transits the star, it will block a fraction  $\delta \approx R^2/R_*^2$  of the star's flux. There will be corrections to this at various points in the transit due to several effects:

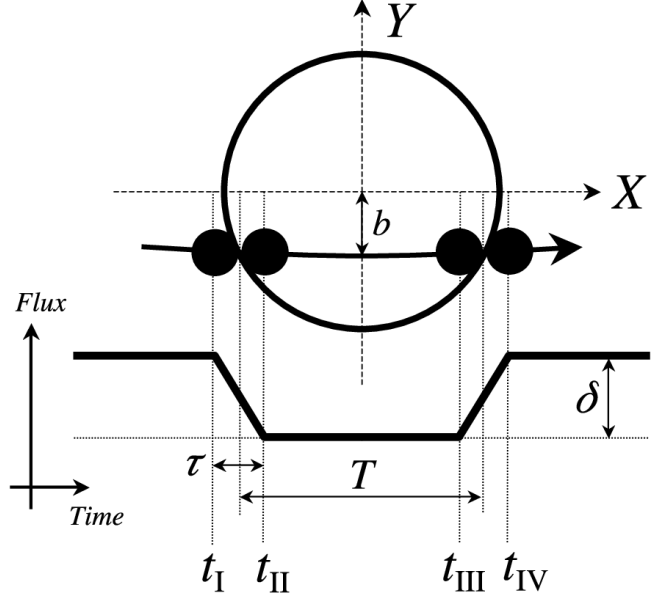


**Figure 2 | Transit Contact Times.** This figure defines the transit times  $t_{\text{I-IV}}$ , the impact parameter  $b$ , and the quantity  $\delta$ .

- During ingress/egress, not all of the planet will be blocking the star
- The outer edges of the stellar disk are darker and redder than the centre, because one sees to a shallower depth into the star when looking at the edges of the disk. As such, the planet may be barely blocking any blue light at all until it reaches near the centre of the disk; conversely the planet is likely blocking IR light all the way across the disk, so transits look sharp in IR but smoother in blue.
- The atmosphere of the planet will preferentially absorb at certain wavelengths, giving  $R$  a “fuzziness”. The transit depth therefore becomes

$$\frac{(R + NH)^2}{R_*^2} \approx \frac{R^2}{R_*^2} + \frac{2NRH}{R_*^2}$$

where the atmospheric scale height  $H = kT/\mu g$  with mean molecular weight  $\mu$ , and  $N$  is typically a few, depending on the wavelength. This correction is very small ( $\sim 10^4$ ), though is larger for hotter planets with inflated atmospheres and large  $H$ .

During occultation, the flux received drops by  $F_p$ . The occultation depth is given by  $F_p/(F_* + F_p) \approx F_p/F_*$ . The form of this will depend on how exactly the planet is emitting its flux. If it is emitting as a blackbody, it will have  $F_p \approx \pi R^2 B(T)$ , and we will have

$$\delta_o = \frac{R^2}{R_*^2} \frac{B(T)}{B(T_*)} \xrightarrow{\lambda \gg hc/kT_*} \frac{R^2}{R_*^2} \frac{T}{T_*}$$

If the planet’s emission is mostly reflected starlight, it will have a luminosity

$$\begin{aligned} L = A \frac{\pi R^2}{4\pi a^2} L_* & \Rightarrow 4\pi R^2 I = A \left( \frac{R}{2a} \right)^2 \cdot 4\pi R_*^2 I_* & \Rightarrow \frac{I}{I_*} = A \left( \frac{R_*}{2a} \right)^2 \\ \Rightarrow \delta_o = \frac{R^2}{R_*^2} \frac{I}{I_*} & = A \left( \frac{R}{2a} \right)^2 \end{aligned}$$

### 2.3.5 Rossiter-McLaughlin Effect

Transits can affect RV measurements. If the star is rotating, the radial velocity (and hence redshift) will vary across the star. When the planet blocks the bluer part of the star, the star will appear redder (on average!) and the spectral lines will get thinner and slump redwards as the bluer parts of the line are blocked; and vice versa when the planet transits the redder part of the star. This manifests in a peak and a trough in an RV profile, which may have different heights if the stellar rotation axis is misaligned with the orbital plane. It turns out this is the case in many stars: the Sun rotates at  $7^\circ$  to the ecliptic; some stars rotate at much higher inclinations.